# Finite Element Modeling of Acoustic Emission Signal Propagation with Various Shaped Waveguides

Andreea Manuela ZELENYAK *, Marvin A. HAMSTAD **, Markus G. R. SAUSE *
* University of Augsburg, Institute for Physics, Augsburg, Germany
** University of Denver, Daniel Felix Ritchie School of Engineering and Computer Science, Denver, CO, USA

**Abstract.** In acoustic emission (AE) technology, when the examination does not allow mounting a sensor directly because of the extreme conditions such as high temperature, chemically environment, insulation, radiation, small or irregular specimens, waveguides are used. Waveguides can have the form of long thin rods or wires usually made of brass, steel or aluminum alloys. The purpose of this research was to investigate the effects of varying waveguide shapes on acoustic emission signal characteristics by means of finite element modeling (FEM). Different designs of an aluminum waveguide are numerically investigated by modeling the acoustic emission signals propagating in a 3 mm thick aluminum plate with the waveguide attached. The signal was generated using a pencil lead break source located on the top of the plate, acting in out-of-plane direction. The modelled signals were evaluated at a distance of 100 mm from the source on the plate surface and on the waveguide. The waveguide was modelled with circular cross-section and an attached segment for sensor mounting. The latter was varied from a simple rectangular cross-section to a conical one. Solid and hollow waveguides filled with air or fluid were investigated. To validate the simulated acoustic emission signal characteristics, experimental signals measured on the plate surface are compared to simulated ones. Waveforms obtained in the simulation process of all waveguides are analyzed. Comparison between each FEM result is presented in terms of the detected signal on the waveguide, time delay between plate surface signal and waveguide signal, mode conversion during waveguide transmission, attenuation in the waveguide and shifts of the signals frequency content.

## 1. Introduction

Innovative non-destructive testing methods such as acoustic emissions (AE) analysis are usually used to identify the stage of material degradation and load history [1,2]. Acoustic emission signals are defined as microscopic displacements of a solid, originating e.g. from crack growth, at the lower ultrasonic frequency range of 20 kHz to 500 kHz [3]. Detection of the AE-signals involved various investigations in the past leading to the most common type of detection systems used in ultrasonic measurements, piezoelectric materials based sensors [4]. Behavior of the piezoelectric sensors detecting in extreme environmental conditions such as high temperature or radiation is well studied and solutions such as using natural crystals instead of ceramic were found. These, and careful selection of the materials

dedicated to cable design and those used for overprotective -braid covering can lead to high purchasing prices for the AE sensors. Piezoceramic lead-zirconate-titanate (PZT) is one common material used for AE sensors with the big inconvenience that it cannot be directly mounted on a structure which operates at high temperatures [5]. A solution to avoid sensor destruction was found by the researchers like Lynnworth et al. and involves usage of thin rods, clad rods or hollow tubes as ultrasonic waveguides (WGs) for detection [6]. Pencil lead break AE signals detected experimentally by a WG mounted sensor were compared with the signals obtained from a plate mounted sensor in terms of signal duplication in the time, frequency and time/frequency domains with good results. Various short WGs with different material properties, length, diameter, face angle were experimentally investigated in order to show the effects upon pulsed events [7,8]. All these experimental investigations involved the usage of more than one WG type leading to high costs and long times to develop the right WG for one measurement purpose. With the increase of the computation power in the past years numerical methods can be used to successfully simulate elastic wave propagation in various materials. In AE testing of thin structures the Lamb waves modes are the most commonly encountered type of guided wave. Often only the fundamental symmetric mode $S_0$ and anti-symmetric mode $A_0$ are present in AE testing [9]. Realistic simulations of guided waves, using finite element method were presented by different researches using software packages like Ansys, Comsol Multiphysics or Abaqus.

The purpose of the current work is to investigate the signal propagation in different shaped thin rods as ultrasonic WGs by finite element simulation, analyzing the influence upon the detected signal's characteristics.

## Modelling of acoustic emission in waveguides

The finite element method (FEM) was used to fulfill this investigation carrying out simulations in Comsol Multiphysics with Structural Mechanics module to solve the constitutive equations for linear-elastic media and piezoelectric media and the AC/DC module for performing a P-SPICE circuit simulation. Simulation of acoustic waves, in particular fundamental anti-symmetric $A_0$ and symmetric $S_0$ Lamb modes using numerical methods was intensively investigated in recent years and results revealed signals which were perfectly reproducing experimental ones [9].

### *1.1 Model setup*

To investigate the effects of WG presence on the acoustic emission characteristics, two full 3-dimensional models were built. The first one involved modeling the propagation of the acoustic emission waves in a simple plate without being influenced by the WG. The signal obtained with this model was kept as reference signal and is called plate conical in the following (pic. 1a). The geometry of the model considers a plate of 600 mm x 600 mm size and 3 mm thickness. As seen in pic. 1a, symmetry boundary conditions along the xz-plane were used to reduce the model dimensions by a factor of two. A monopole source PLB was chosen to be acting in out-of-plane direction at (x,y,z)=(0,0,3) mm, located at the middle of the plate. At the detection point at (x,y,z)=(100,0,3) mm a conical sensor was modeled to avoid interference with incident reflections within the duration time of the simulation. The sensor model was previously studied numerically by Sause et al. and all parameters used are the same [9] (pic.1c).

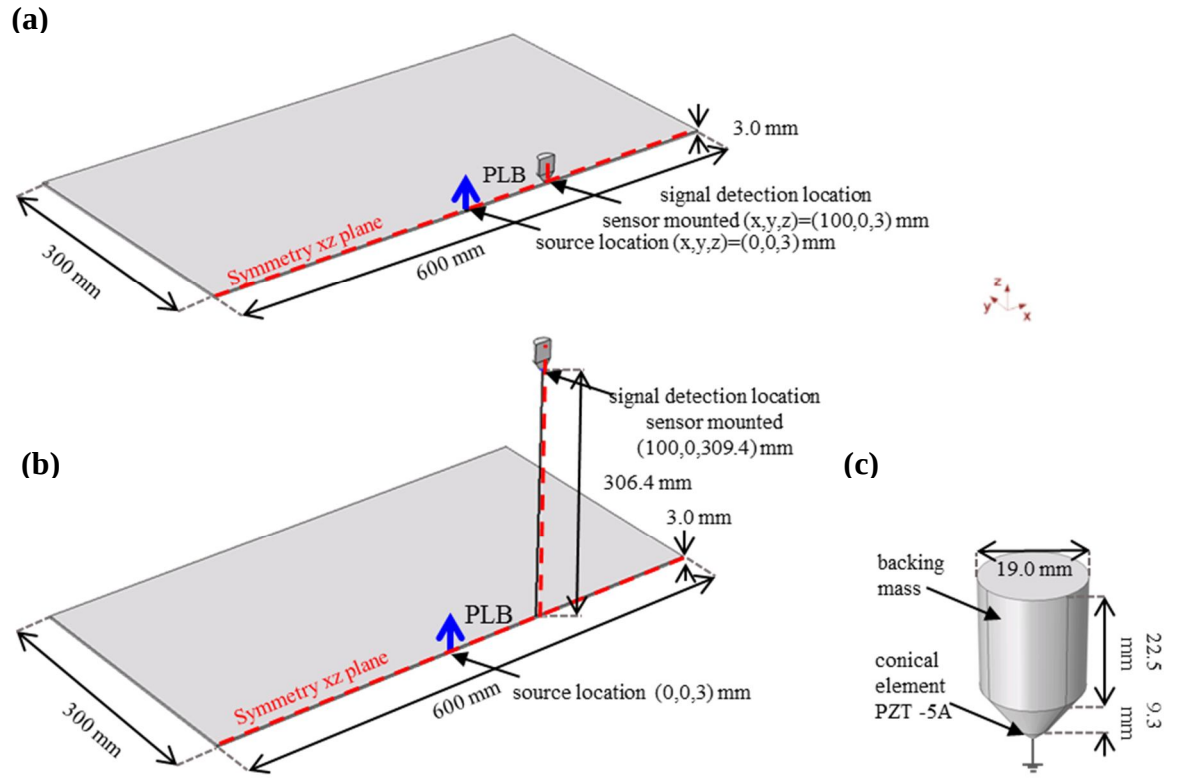


**Pic.1** Model geometry for the (a) plate with conical sensor (b) plate with waveguide and conical sensor [9] and (c) details of the conical sensor model

The second 3-dimensional model plate had the same geometry as the reference one, but at the detection point, between the plate and the sensor, differently shaped WGs were introduced (pic. 1b). A total number of seven types of WGs were investigated. The WGs length was kept constant at 306.4 mm with a small diameter of 1.59 mm following the experimental used geometry by Hamstad [7]. In the following only the upper and the lower parts of the WGs were changed in shape.

Most of the WGs were solid rods with shape adjustments at the two ends (cf. pic 2a).

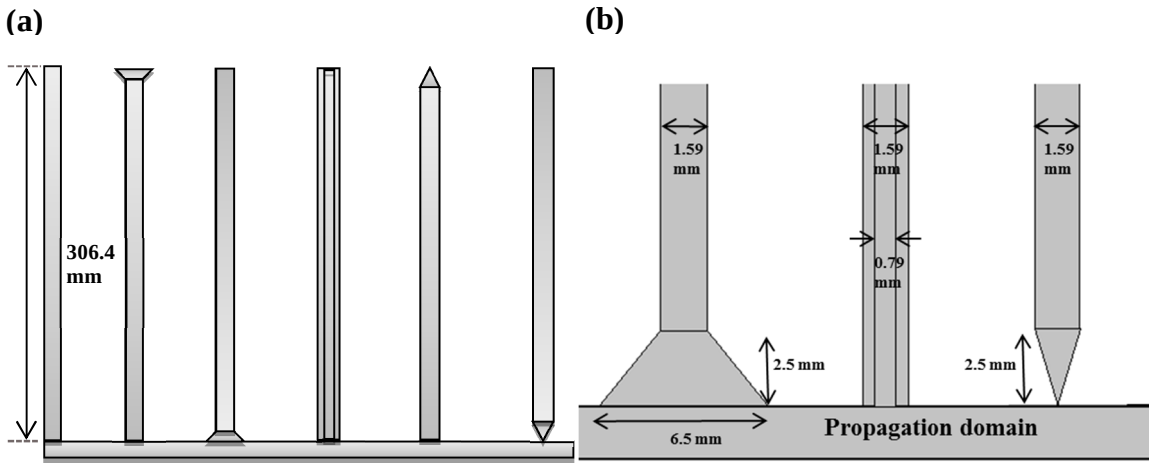


**Pic.2** Waveguide geometries of different cases (a) and detailed view of ends (b).

A 2.5 mm sub-section at either end of the total 306.4 mm length was replaced with various shapes for the study. From a cylindrical shape, the sub-section was changed to conical with a large bottom radius of 3.25 mm and a semi-angle of 45° generating two study cases. Another variation considers a conical sub-section with a very small bottom

radius 0.8 mm a semi-angle of 17° creating two more cases, so called sharpened WGs. In addition, two special cases were built using hollow WGs, with the inner diameter of 0.79 mm being half of the total WG's diameter, filled with air or water. The different geometry variations are illustrated in pic. 2a, with a detailed view given in pic. 2b.

The material for the propagation domain and for the WGs was $AlMg_3$ for all cases with properties shown in table 1, with the elastic properties taken from [10].

**Table1.** Elastic properties of the materials used in FEM cases.

| **Property** | **$AlMg_3$** |
|---|---|
| Density[kg/m$^3$] | 2660 |
| Elastic modulus [GPa] | 70 |
| Poisson ratio | 0.33 |

The expected waves to develop in the plate and further transmitted into the waveguide are Lamb wave modes of fundamental order due to the small thickness of the plate.

Due to the fact that the WGs were mounted perpendicular to the plate, the flat end of the WG is expected to be excited only by the out-of-plane displacement as pointed out by Hamstad in [7]. The differences can be given by the viscous couplant which is usually used in experiments and which in this investigation was not modeled.

Convergence of the numerical solution was previously investigated through a series of models developed specifically to create an efficient mesh and temporal resolution for modeling pencil lead break waves in large structures. Numerical studies conducted so far in this field by other authors showed that having a mesh resolution of 1 mm maximum element size and signals calculated with $1\times10^{-7}$ s time step will lead to a convergent solution. Our researches concerning the convergence of the solution revealed that it is sufficient to have 1mm mesh resolution along a line of interest using a distribution of the mesh size for the rest of the plate within the interval [1 to 3] mm. Mesh elements are of cubic geometric shape order. A time step of $1\times10^{-7}$ s was used to calculate a total length of 100 μs of signal propagation, extended to 150 μs in WGs cases. For an accurate model of the sensor a mesh resolution in the interval of [0.4 to 0.5] mm size was used with a coherence level $\geq$0.99801 as demonstrated by [9].

## 2. Comparison between Simulation and Experiment

A validation of the simulation approach was done by comparing the modeled plate conical signal to an experimental signal obtained by Hamstad in his research upon small diameter waveguide usage in AE [7]. The sensor used is a wideband conical one, produced at the National Institute of Standards and Technology (NIST) Colorado, which was previously described in two publications [13,14]. The conical element has 1.5 mm aperture and 2.5 mm height, with the piezoelectric material being PZT 5A. The conical element, the backing mass, a small part of the case and the preamplifier were modeled. This was found to be sufficient to obtain a signal similar to the experimental one. The experimental setup also contains a plate made from an aluminum alloy with 3.1 mm thickness, as propagation medium and a PLB source with 0.3 mm diameter and 2H hardness to generate the AE signals. For the modeling work we used the material properties of table 1. A cosine bell function with the excitation time of $1\times10^{-6}$ s and a maximum force of 3 N simulates the pencil lead break behavior as acoustic emission source acting in the out-of-plane direction on the plate surface. The geometry of this model was similar with the one presented in pic. 1a, the differences being given by presence of the sensor model at the detection point at 254 mm distance and the total plate width of 550 mm x 500 mm with 3.1 mm thickness.

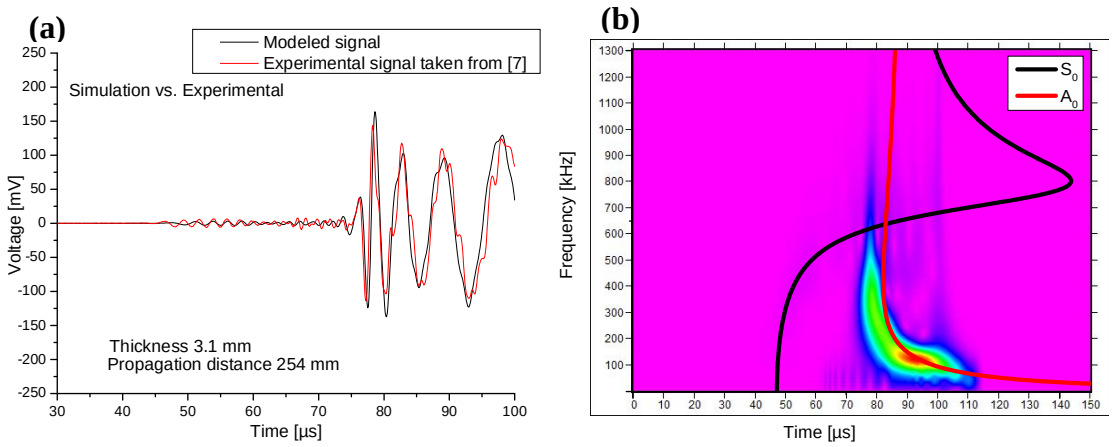


**Pic. 3** Comparison between simulated and experimental signal (a) and wavelet transformation of the simulated signal with superimposed dispersion curves (b)

The experimental signal was directly compared with the simulated voltage signal. The dominating modes due to the PLB out-of-plane source applied to the surface of the plate are the $A_0$ mode with a weak contribution of the $S_0$ mode in the beginning of the signal [15]. The shape of the experimental signal, as shown in pic. 3, is well reflected by the simulated signal. There are minor differences in arrival time due to the fact that the exact properties of the experimentally used aluminum alloy are unknown. Small discrepancies in the magnitude can also be observed. The latter can be attributed to the attached circuitry which models cables and preamplifier components, as demonstrated by Sause et al. in [9]. For this simulation we choose 5 Ω resistance of the connection cables and 15 pF capacitance and for the preamplifier 10 MΩ and 20 pF capacitance. Variation of the cable capacitance values can lead to a better match in terms of magnitude. In pic. 3b the Wavelet transformation (WT) of the simulated signal using the AGU Vallen software is compared to the theoretical $A_0$ and $S_0$ dispersion curves calculated for aluminum for a propagation distance of 254 mm. The WT also reveals good agreement between the dispersion curves and the simulated signal.

## 3. Results and discussions

### *3.1 Post processing*

In the following, simulation results of the cases are compared to each other and are discussed in terms of observations from literature.

In order to discuss comparable signals spectra all simulated signals undergo a series of post processing steps:

- The WG signal was shifted forward in time to superimpose (e.g. for the rectangular cross section waveguide by 60.2 µs)
- All signals from the plate and WG conical sensors were terminated at a convenient zero
- All signals were extended with 0 values to a total length of 2048 points
- The Fast Fourier Transformation (FFT) were calculated with a square window function
- The resulting FFTs were smoothed by a 30 point Savitsky-Golay ($5^{th}$ polynomial) method
- The FFT results were adjusted to superimpose from 0 to 100 kHz in order to fit and compare

Waveforms of simulated signals after 100 µs of propagation distance are shown in pic. 4. The reference signal shows the arrivals of $S_0$ and $A_0$ modes after 20.5 µs and 32.4 µs, respectively.

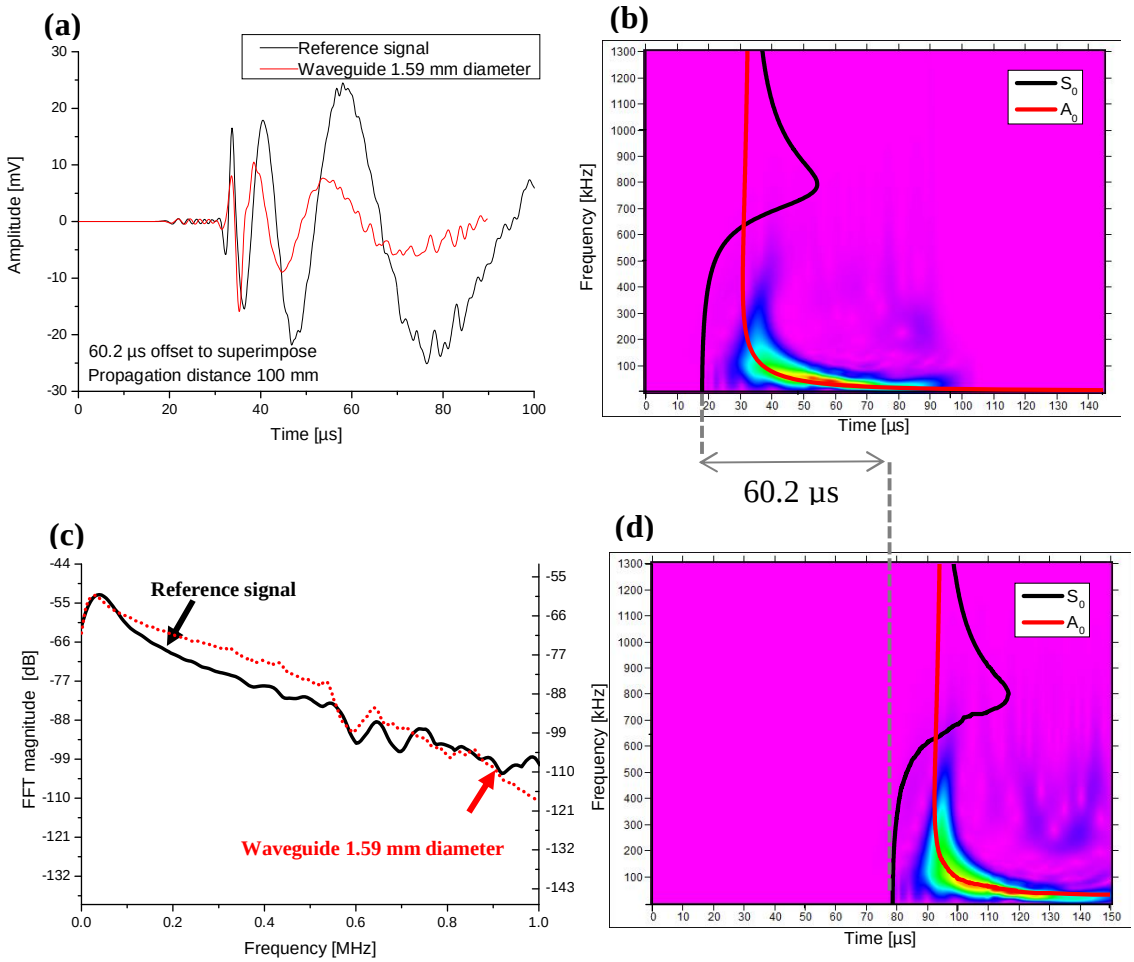


**Pic. 4** Waveform signals from reference signals and WG with circular cross section (a) WT of reference signal (b) frequency spectra of both signals (plate conical left vertical axis) (c) and WT of waveguide signal (d).

The time domain signal of the reference case (detected directly on the plate) and detected on the waveguide is presented in pic. 4a. The time offset deduced from the simulation results is 60.2 µs and is in good agreement with the experimental results which revealed 60.4 µs time delay between the signal detected on the plate and the signal detected by the conical sensor on top of the WG [7]. The WT of the two signals are presented in pics. 4b and 4d, respectively. Both signals exhibit a clear presence of $A_0$ and $S_0$ modes. The frequency content of the signals is compared after the post processing steps mentioned above were applied on both signals. The frequency curves presented in pic. 4c shows that the signals are qualitatively similar also in the frequency domain after a reduction in amplitude of the reference signal by with 7.4 dB to fit the WG signal

*3.2 Waveguide shape influence*

In order to see the influence of the WG shape on the frequency content of the detected signals we compare the Fast Fourier transformation results. The frequency spectra resulted curves are shown in pic. 5a. with the same magnitude scale. A first comparison is made in terms of magnitude offset between the reference plate signal and the signals detected by the WG mounted sensor.

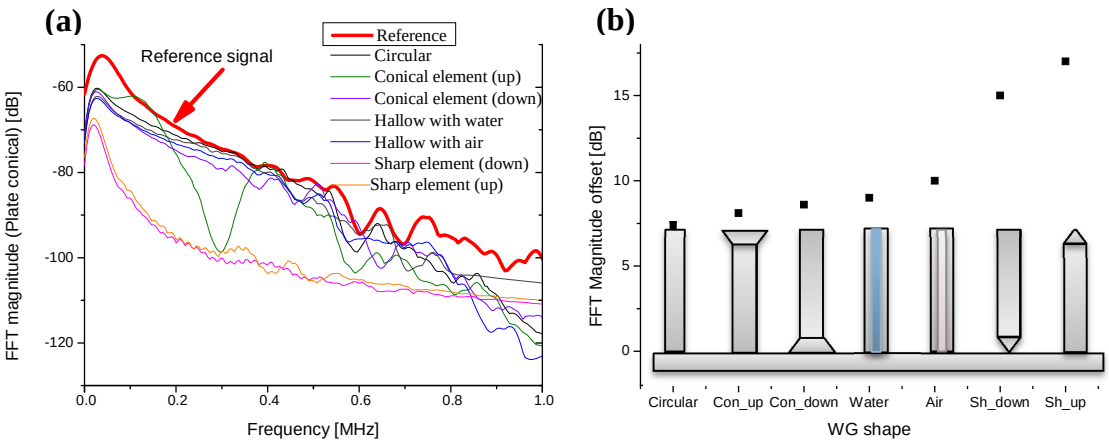


**Pic.5** Frequency spectra a) plate conical reference case and 1.59 mm Al waveguide circular cross section b) magnitude vs. shape

The magnitude offset of 7.4 dB corresponds to the circular cross section WG signal and it is the lowest magnitude difference obtained amongst all geometrical implementations investigated (cf. pic.5b). Examination of the signals detected by the different geometries shows clear differences between the magnitudes of the WG signals in comparison with the reference signal. The WGs with sharp tips revealed to have the highest impact on the transmitted amplitudes, independent if the sharp sub-section was place on the lower end or the upper end. This could be probably due to small aperture of the WG. This effect was already pointed out by Sause et al. in the work concerning sensor modeling highlighting the tendency to increase the amplitude of the detected signal when the sensor diameter was increased [9]. The amplitude of the WG with sharp edge at the upper end was down with additional 9.6 dB compared to the circular cross section WG and with 17 dB compared to the reference signal (cf. pic.5b). A high amplitude decrease manifests also in the WG with conical attachments in the [0.2 to 0.4] MHz frequency range. Overall the FFTs of the other WGs signals are qualitatively similar and there were no mode conversions noticed in all cases investigated.

The special cases in which hollow WGs were used did not show any noticeable deviations to the duplicated signal, when compared to the reference signal. The air filled WG showed a decrease in magnitude compared with the circular WG, 2.6 dB offset between them, while the signal had the same arrival time and same qualitative shape. When the air was replaced with water the magnitude offset was smaller, 1.6 dB magnitude offset, but a delay of 3.4 µs in arrival time was noticed.

## 4. Conclusion

Through this numerical investigation it has been demonstrated that finite element modeling can be used to successfully simulate signal propagation in WGs. The multiphysics coupling provided by the Comsol environment was used in this approach to model piezoelectric conversion and the attached electric circuit for sensor implementation. The validation of the models was carried out using a comparison to the experimental AE signal obtained by Hamstad [7].

Simulating different designs of the aluminum waveguides has shown that the WG geometry can have a significant impact on transmission of the Lamb waves propagating in the plate investigated in terms of arrival times or magnitude shifts in the frequency spectrum. It has been shown through time domain signals and also frequency spectra that

WGs are capable to duplicate the out-of-plane displacement of the plate which can be detected at the WG end by an attached wideband sensor. Such duplication using WGs was already demonstrated experimentally but with the help of such modeling work the influence of new geometries and WG materials can suitably be predicted.

Further numerical investigations concerning WGs usage in acoustic emission detection can be extended to studies involving environmental changes in terms of temperature, signal attenuation studying different evaluation distances or other parameters influencing WG transmission like diameter, length or impedance mismatches.

## References


[1] E H Saenger, G K Kocur, R Jud, M Torrilhon, 'Application of time reverse modeling on ultrasonic non-destructive testing of concrete', Applied Mathematical Modelling, Vol 35, pp. 807–816, 2011.

[2] C U Grosse, M Ohtsu, 'Acoustic Emission Testing: Basics for Research – Applications in Civil Engineering'; With Contributions by Numerous Experts, Springer, Heidelberg, ISBN 978-3-540-69895-1, 2008.

[3] M G R Sause, 'Identification of failure mechanisms in hybrid materials utilizing pattern recognition techniques applied to acoustic emission signals', PhD Dissertation, Augsburg (Germany), Augsburg University, 2010.

[4] E S Boltz, C M Fortunko, M A Hamstad, M C Renken, 'Absolute sensitivity of air, light and direct-coupled wideband acoustic emission transducers', Review of Progress in Quantitative Nondestructive Evaluation, vol. 14, Plenum Press, New York, pp. 967–974, 1995.

[5] Ian T. Neilla, I. J. Oppenheima, D W Greveba , 'A Wire-Guided Transducer for Acoustic Emission Sensing', Proceedings of the SPIE, Volume 6529, article id. 652913, 2007.

[6] L Lynnworth, Yi Liu, and J. Umina, 'Extensional Bundle Waveguide Techniques for Measuring Flow of Hot Fluids', IEEE Transactions on Ultrasonics, Ferroelectrics, and Frequency Control, Vol. 42, No. 4, 538-544, 2005.

[7] M A Hamstad, 'Small diameter waveguide for wideband acoustic emission', Journal of Acoustic Emission Vol. 24, pp. 234-247, 2006.

[8] J Sikorska and J Pan, 'The effect of waveguide material and shape on acoustic emission transmission characteristics Part 1: traditional features', Journal of Acoustic Emission Vol. 22, pp. 264-273, 2004.

[9] M G R Sause, M. A. Hamstad, S. Horn, 'Finite element modeling of conical acoustic emission sensors and corresponding experiments', Sensors and Actuators A 184, pp. 64– 71, 2012.

[10] M G R Sause , S. Horn, 'Influence of internal discontinuities on ultrasonic signal propagation in carbon fiber reinforced plastics',30th European Conference on Acoustic Emission Testing & 7th International Conference on Acoustic Emission University of Granada, 12-15 September 2012.

[11] M G R Sause, 'Investigation of pencil-lead breaks as acoustic emission sources', Journal of Acoustic Emission 29, pp. 184-196, 2011.

[12] Y Gharaibeh1, S Soua, G. Edwards, P. Mudge, W Balachandran, 'Modelling guided waves in complex structures - Part 2: Wire bundles - with and without insulation', paper presented at NDT 2009, Blackpool, UK, 15-17 Sept. 2009.

[13] M A Hamstad, C.M. Fortunko, 'Development of Practical Wideband High Fidelity Acoustic Emission Sensors', Nondestructive Evaluation of Aging Bridges and Highways, Proc. SPIE 2456, pp. 281-288, 1995.

[14] M A Hamstad, 'Improved Signal-to-Noise Wideband Acoustic/Ultrasonic Contact Displacement Sensors for Wood and Polymers', Wood and Fiber Science, 29 (3), pp. 239-248, 1997.

[15] M A Hamstad, 'On lamb modes as a function of acoustic emission source rise time, Journal of Acoustic Emission' 28, pp. 41–58, 2010.